

A Nonsense Mutation in a Cinnamyl Alcohol Dehydrogenase Gene Is Responsible for the Sorghum *brown midrib6* Phenotype^{1[W][OA]}

Scott E. Sattler*, Aaron J. Saathoff, Eric J. Haas, Nathan A. Palmer, Deanna L. Funnell-Harris, Gautam Sarath, and Jeffrey F. Pedersen

Grain, Forage, and Bioenergy Research Unit, United States Department of Agriculture-Agricultural Research Service (S.E.S., A.J.S., N.A.P., D.L.F.-H., G.S., J.F.P.), Department of Agronomy and Horticulture (S.E.S., A.J.S., N.A.P., G.S., J.F.P.), and Department of Plant Pathology (D.L.F.-H.), University of Nebraska, Lincoln, Nebraska 68583-0739; and Department of Chemistry, Creighton University, Omaha, Nebraska 68178 (E.J.H.)

brown midrib6 (*bmr6*) affects phenylpropanoid metabolism, resulting in reduced lignin concentrations and altered lignin composition in sorghum (*Sorghum bicolor*). Recently, *bmr6* plants were shown to have limited cinnamyl alcohol dehydrogenase activity (CAD; EC 1.1.1.195), the enzyme that catalyzes the conversion of hydroxycinnamoyl aldehydes (monolignols) to monolignols. A candidate gene approach was taken to identify *Bmr6*. Two CAD genes (Sb02g024190 and Sb04g005950) were identified in the sorghum genome based on similarity to known CAD genes and through DNA sequencing a nonsense mutation was discovered in Sb04g005950 that results in a truncated protein lacking the NADPH-binding and C-terminal catalytic domains. Immunoblotting confirmed that the Bmr6 protein was absent in protein extracts from *bmr6* plants. Phylogenetic analysis indicated that Bmr6 is a member of an evolutionarily conserved group of CAD proteins, which function in lignin biosynthesis. In addition, Bmr6 is distinct from the other CAD-like proteins in sorghum, including SbCAD4 (Sb02g024190). Although both *Bmr6* and *SbCAD4* are expressed in sorghum internodes, an examination of enzymatic activity of recombinant Bmr6 and SbCAD4 showed that Bmr6 had 1 to 2 orders of magnitude greater activity for monolignol substrates. Modeling of Bmr6 and SbCAD4 protein structures showed differences in the amino acid composition of the active site that could explain the difference in enzyme activity. These differences include His-57, which is unique to Bmr6 and other grass CADs. In summary, *Bmr6* encodes the major CAD protein involved in lignin synthesis in sorghum, and the *bmr6* mutant is a null allele.

Plant cell walls constitute a vast reserve of fixed carbon. Cellulose and lignin are the first and second most abundant polymers on the planet, respectively (Jung and Ni, 1998). The world community has started to look to biomass as substrates for plant-based biologically sustainable fuels, which would mitigate carbon dioxide emission and reduce petroleum dependence (Sarath et al., 2008; Schmer et al., 2008). In the current generation of biofuels, ethanol is being

synthesized via the fermentation of grain starch or sugarcane juice. For the next generation of biofuels, research is being directed toward the conversion of lignocellulosic biomass into biofuels (Chang, 2007). As bioenergy technologies progress, the conversion of biomass to biofuels could involve a range of chemical, biochemical, and fermentation processes to produce biofuels; alternate biofuels, such as butanol or dimethylfuran, are also on the horizon (Ezeji et al., 2007; Roman-Leshkov et al., 2007). Most liquid biofuel production processes will likely rely on the conversion of the cell wall polysaccharides cellulose and hemicellulose into monomeric sugars.

Plant cell walls consist of a complex polysaccharide moiety composed of cellulose microfibrils, composed of β -1,4-linked Glc polymers (Carpita and McCann, 2000). Connecting the cellulose microfibrils to each other is a hemicellulose network, whose structure and composition are species dependent, and which is mainly composed of glucuronoarabinoxylans in grasses (Carpita and McCann, 2000). Lignin, a nonlinear heterogeneous polymer derived from aromatic precursors, cross-links these polysaccharides, rigidifying and reinforcing the cell wall structure (Carpita and McCann, 2000). The addition of lignin polymers to the polysaccharide matrix creates a barrier that is chemically and microbially resistant.

¹ This work was supported by U.S. Department of Agriculture-Agricultural Research Service Project 5440-21220-024-00D and Office of Science (Office of Biological and Environmental Research), U.S. Department of Energy Grant DE-FG02-07ER64458 (S.E.S. and J.F.P.). Mention of trade names or commercial products in this publication is solely for the purpose of providing specific information and does not imply recommendation or endorsement by the U.S. Department of Agriculture.

* Corresponding author; e-mail scott.sattler@ars.usda.gov.

The author responsible for the distribution of materials integral to the findings presented in this article in accordance with the policy described in the Instructions for Authors (www.plantphysiol.org) is: Scott E. Sattler (Scott.Sattler@ars.usda.gov).

[W] The online version of this article contains Web-only data.

[OA] Open access articles can be viewed online without a subscription.

www.plantphysiol.org/cgi/doi/10.1104/pp.109.136408

Lignin can block the liberation of sugars from the cell wall polysaccharide moieties, release compounds that can inhibit microbes used for fermenting sugars to fuels, and adhere to hydrolytic enzymes. Understanding lignin synthesis, structure, and function to increase cell wall digestibility has long been a goal for forage improvement and paper processing (Mackay et al., 1997; Jung and Ni, 1998). Recently, manipulating lignin has also become an important target for bioenergy feedstock improvement (Chen and Dixon, 2007; Li et al., 2008).

Lignin is derived from the phenylpropanoid pathway and contains primarily three types of phenolic subunits: *p*-hydroxyphenyl, guaiacyl, and syringyl units (Dixon et al., 2001). The phenolic aldehyde precursors are reduced into their corresponding alcohols (monolignols) and subsequently transported to the cell wall (Fig. 1), where laccases and peroxidases catalyze lignin polymerization through the formation of monolignol radicals (Boerjan et al., 2003). Therefore, most research efforts to manipulate lignin have focused on biosynthesis of the monolignols. Most of the enzymes involved in monolignol synthesis have been cloned and characterized in *Arabidopsis* (*Arabidopsis thaliana*) and other dicot species, using both mutagenic and transgenic approaches to study the impact of these gene products on dicot cell walls (Anterola and Lewis, 2002). However, there are significant differences in the architecture, polysaccharide composition, and phenylpropanoid composition of grass cell walls compared

with those of dicots (Carpita and McCann, 2000; Vogel and Jung, 2001). For example, grasses contain significant amounts of *p*-coumaric acid and ferulic acid that are cross-linked to cell wall polysaccharides through ester and ether linkages in addition to their presence in lignin (Grabber et al., 1991; Boerjan et al., 2003). Because many of the proposed dedicated bioenergy crops are grasses, there is a need to identify and understand the function of the gene products involved in lignin biosynthesis in these species (Vermerris et al., 2007; Li et al., 2008; Sarath et al., 2008).

The brown midrib phenotype has been useful for identifying mutants affecting lignin synthesis in grasses because it is a visible phenotype. Spontaneous brown midrib mutants were first discovered in maize (*Zea mays*; Jorgenson, 1931) and were subsequently generated in sorghum (*Sorghum bicolor*) using diethyl sulfate mutagenesis (Porter et al., 1978). Brown midrib mutants in maize, sorghum, and pearl millet (*Pennisetum glaucum*) have increased forage digestibility for livestock (Cherney et al., 1990; Akin et al., 1993; Jung et al., 1998; Oliver et al., 2004). In maize and sorghum, there are at least four brown midrib loci in their respective genomes (Jorgenson, 1931; Porter et al., 1978; Gupta, 1995). The genes encoding *bm3* in maize and *bmr12* in sorghum are the only loci cloned to date, and both encode highly similar caffeic acid *O*-methyl transferases (Vignols et al., 1995; Bout and Vermerris, 2003). A second brown midrib locus associated with reduced cinnamyl alcohol dehydrogenase (CAD) activity has been identified both in maize (*bm1*; Halpin et al., 1998) and sorghum (*bmr6*; Bucholtz et al., 1980; Pillonel et al., 1991). CAD is a member of the alcohol dehydrogenase superfamily of proteins that catalyzes the conversion of the hydroxycinnamoyl aldehydes into alcohols prior to their incorporation into lignin polymers (Fig. 1). Reduced CAD activity results in increased digestibility on dry weight basis, altered cell wall architecture, reduced lignin level, and the incorporation of phenolic aldehydes into lignin in sorghum and maize (Pillonel et al., 1991; Provan et al., 1997; Halpin et al., 1998; Marita et al., 2003; Shi et al., 2006; Palmer et al., 2008). The reduced CAD activity in *bm1* has been genetically mapped to a region of the maize genome that contained a CAD gene, *ZmCAD2* (Halpin et al., 1998), but a mutation was not identified. However, it has recently been shown that *bm1* down-regulated the expression of several lignin biosynthetic genes, suggesting its gene product may be a regulatory protein (Shi et al., 2006; Guillaumie et al., 2007).

To identify the mutation responsible for the *bmr6* phenotype and to characterize how *bmr6* impacts the lignin biosynthetic pathway, a candidate gene approach was taken. Here, we describe the cloning and characterization of *Bmr6* and a related protein, *SbCAD4*. The identification and characterization of *Bmr6* has revealed the major monolignol CAD protein in the grasses, which is likely to aid the development of new strategies to increase conversion of sorghum and other grass feedstocks to biofuels.

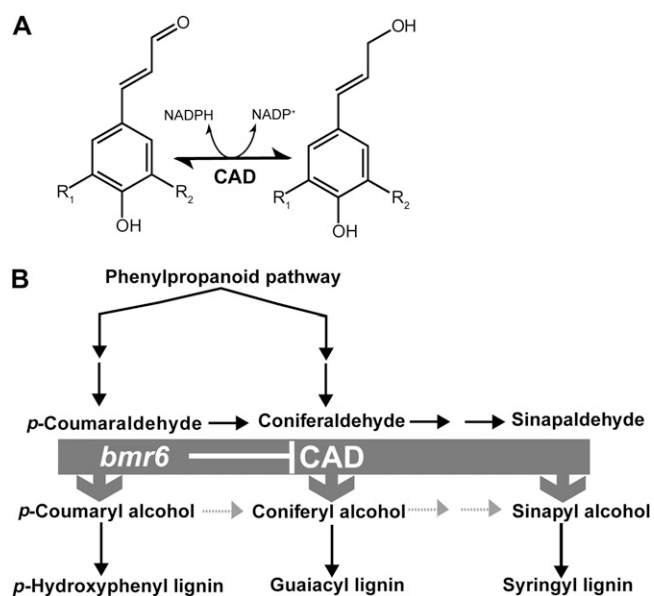


Figure 1. The CAD enzyme and its role in the monolignol biosynthetic pathway. **A**, CAD catalyzes the conversion of cinnamyl aldehydes to alcohols using NADPH as its cofactor. *p*-Coumaryl aldehyde and alcohol, R₁ and R₂ = H; caffeoyl aldehyde and alcohol, R₁ and R₂ = OH; coniferyl aldehyde and alcohol, R₁ = H and R₂ = OCH₃; sinapyl aldehyde and alcohol, R₁ and R₂ = OCH₃. **B**, A simplified model of the lignin biosynthetic pathway where CAD catalyzes the final step in monolignol biosynthesis.

RESULTS

Lignin Composition

To examine the lignin composition in *bmr6* relative to the wild type, thioacidolysis was performed on the stalks of mature Atlas plants, and the products were analyzed by gas chromatography-mass spectrometry (GC-MS; Fig. 2). There was a significant reduction in all three main lignin subunits, H-, G-, and S- lignin: 4.8-, 7.3-, and 17.7-fold, respectively, relative to the wild type. The most significant reduction was in S-lignin, which led to a reduced S:G ratio (Fig. 2A). Two minor lignin subunits, S-indene and G-indene, were elevated 9.5- and 8.3-fold, respectively, in *bmr6* relative to the wild type (Fig. 2B). The indene subunit resulted from the incorporation of cinnamyl aldehydes into the lignin polymer in place of cinnamyl alcohols. These results were consistent with previous analyses of lignin composition in *bmr6* in other sorghum varieties, which indicated that *bmr6* appeared to have a

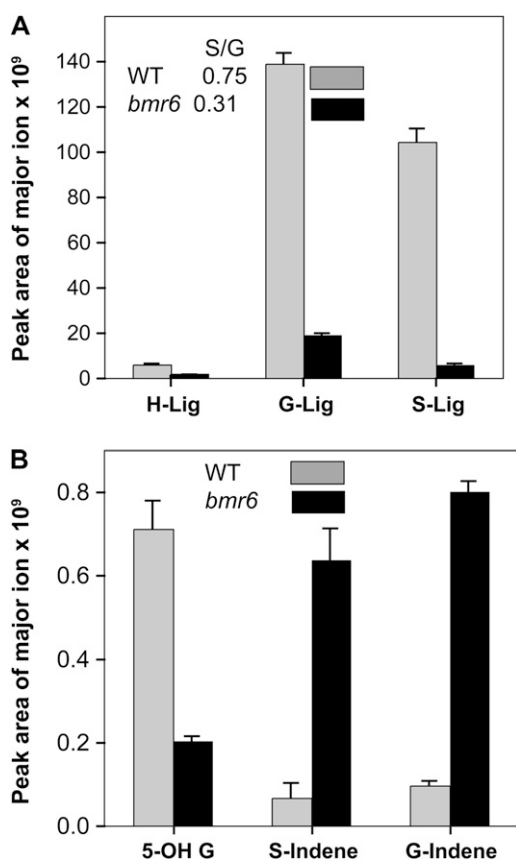


Figure 2. Lignin composition in *bmr6* and the wild type (WT). A, Distribution of major lignin subunits in stems of Atlas wild type and *bmr6* were quantified by GC-MS following thioacidolysis. B, Minor lignin subunits were determined by abundance of ions diagnostic of 5-OHG-lignin, S-indene, and G-indene in Atlas stems. Data are the pooled means (\pm SE) of triplicate analyses from two independent extractions

deficiency in CAD activity (Pillonel et al., 1991; Palmer et al., 2008).

Identification of *bmr6*

Because it had previously been shown that CAD activity was reduced in *bmr6* whole plants (Pillonel et al., 1991), or not detected in young *bmr6* internodes (Palmer et al., 2008), a candidate gene approach was taken to identify the gene encoding *bmr6*. The draft of the sorghum genome was searched using the tBLASTN algorithm and queried with the amino acid sequences of *AtCAD4* and *AtCAD5*, the CAD genes demonstrated to be involved in monolignol biosynthesis in Arabidopsis (Kim et al., 2004; Sibout et al., 2005). The search identified two genes in the sorghum genome, Sb04g005950 and Sb02g024190, whose predicted amino acid sequences shared significant similarity to the Arabidopsis proteins *AtCAD4* (67.7% and 83.4%) and *AtCAD5* (68.4% and 82.5%), respectively. A tBLASTN search of the nonredundant GenBank database was performed using the predicted amino acid sequences of both Sb02g024190 and Sb04g005950 as the query sequences. The search revealed that Sb04g005950 was highly similar to the maize *ZmCAD2* sequence (97.8%), which is the map location of *Bm1*. PCR primers were designed to amplify the genomic and cDNA sequences of Sb04g005950. The genomic DNA sequences for Sb04g005950 were amplified and sequenced from *bmr6* and wild-type near-isogenic lines in three different backgrounds: Atlas, Wheatland, and RTx430. The cDNA sequences for Sb04g005950 were amplified by RT-PCR and sequenced from *bmr6* and wild-type plants in Atlas and Wheatland near-isogenic lines.

Both the genomic and cDNA sequences of Sb04g005950 indicated that a C-to-T transition mutation was present in *bmr6* but not in any wild-type sequence. This mutation changed amino acid 132 of the protein from Gln (CAG) to a stop codon (UAG; Fig. 3). The C-to-T transition identified in *bmr6* is consistent with the mutagen diethyl sulfate used to treat the population from which *bmr6* was isolated (Bignami et al., 1988). The *bmr6* sequence encodes a predicted truncated protein that lacks the nucleotide binding (NADPH) and C-terminal catalytic domains (Supplemental Fig. S1); hence, *bmr6* is presumably a null allele. These results are consistent with the previously observed lack of CAD activity in *bmr6* (Palmer et al., 2008).

To further verify that the C-to-T transition mutation was present in *bmr6* accessions and not in wild-type accessions, a cleaved-amplified polymorphic sequence (CAPS) marker for *Bmr6* was designed (see "Materials and Methods"). The C-to-T transition mutation introduced a *Bsa*AI restriction site in *bmr6*. Following PCR amplification, restriction digest with *Bsa*AI cleaved the fragment amplified from *bmr6*, but not the wild-type amplification product (Fig. 3B). This PCR-based marker should be useful for future bioenergy research

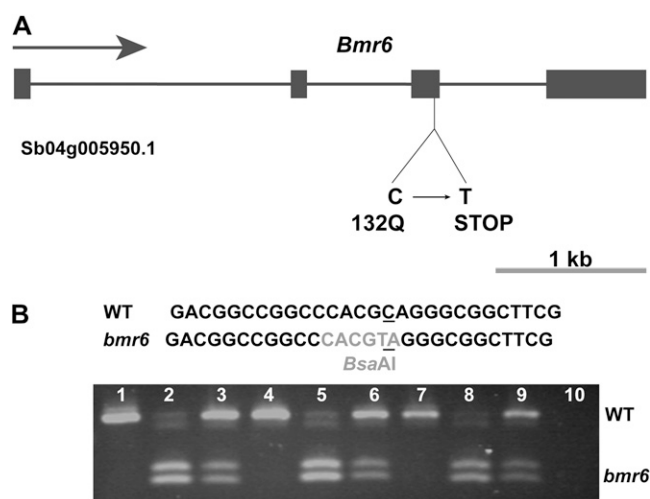


Figure 3. *Bmr6* locus and *bmr6* mutation. A, The gene structure of the *Bmr6* gene, which is located on chromosome 4. The exons are indicated as solid boxes, and the introns are indicated as lines. B, CAPS marker for *Bmr6* locus was designed to verify mutation. PCR primers were used to amplify a 613-bp fragment of *Bmr6* from sorghum genomic DNA. The amplification products were digested with the restriction enzyme *Bsa*I and analyzed by agarose gel electrophoresis. The C-to-T transition mutation in *bmr6* created a *Bsa*I restriction site. The wild-type (WT) DNA sequence is not cleaved by *Bsa*I, but the *bmr6* sequence is, resulting in two fragments of 333 and 280 bp. het, Heterozygote is 1:1 mixture of wild-type and *bmr6* genomic DNA. Lane 1, Atlas wild type; lane 2, Atlas *bmr6*; lane 3, Atlas het; lane 4, R Tx430 wild type; lane 5, R Tx430 *bmr6*; lane 6, R Tx430 het; lane 7, B Wheatland wild type; lane 8, B Wheatland *bmr6*; lane 9, B Wheatland het; lane 10, no DNA negative control.

and breeding efforts using *bmr6* because plants can be screened at early stages and the marker is codominant, so heterozygous plants can be identified. This polymorphic restriction site was present in the near-isogenic lines Atlas *bmr6*, RTx430 *bmr6*, and Wheatland *bmr6* and was absent from wild-type Atlas, RTx430, and Wheatland (Fig. 3B). Because each near-isogenic line was constructed selecting for brown midrib phenotype (prior to the identification of the *bmr6* mutation) and was backcrossed to parental background (Atlas, Tx430, and Wheatland) for four cycles, 93.75% of the genome is backcrossed parent (Pedersen et al., 2006a, 2006b). In addition, no other CAD genes are present on chromosome 4, aside from the *Bmr6* (Sb04g005950.1) locus. The probability that a mutation in another region of the genome is responsible for the *bmr6* phenotype is 0.000244; therefore, the mutation identified in the *Bmr6* (Sb04g005950.1) locus is almost certainly responsible for *bmr6* phenotype.

Phylogenetic Analysis

To compare *Bmr6* and *SbCAD4* with other CAD protein sequences in sorghum and other plants, predicted amino acid sequences were obtained from public databases and a phylogenetic tree was constructed.

Included in the analysis were CAD sequences whose function in monolignol biosynthesis has been demonstrated and previously published from loblolly pine (*Pinus taeda*; PtCAD; Mackay et al., 1995; Ralph et al., 1997), Arabidopsis (AtCAD and AtCAD5; Kim et al., 2004; Sibout et al., 2005), tobacco (*Nicotiana tabacum*; NtCAD19; Knight et al., 1992; Halpin et al., 1994), aspen (*Populus trichocarpa*; PotCAD; Li et al., 2001), and eucalyptus (*Eucalyptus gunnii*; EgCAD2; Goffner et al., 1992; Grima-Pettenati et al., 1993). Five other sorghum sequences with similarity to *Bmr6* and *SbCAD4* were obtained by tBLASTN searches of the sorghum genome database. Sequences similar to *Bmr6* were also obtained from the green algae *Chlamydomonas reinhardtii*, the moss *Physcomitrella patens*, and the lycophyte *Selaginella moellendorffii* genome projects through the tBLASTN algorithm. Neither *Chlamydomonas* nor *Physcomitrella* is known to synthesize lignin; hence, these proteins are unlikely to function as CADs. *Selaginella* is a primitive vascular plant and one of earliest extant organisms that synthesizes lignin. The Arabidopsis CAD and CAD-like sequences were included because the Arabidopsis genome is one of the best characterized in plants and these proteins have been extensively studied.

The phylogenetic tree indicated that all CADs known to be involved in monolignol biosynthesis were found in a single clade (Fig. 4). These CADs are referred to as CAD2, after the original member identified from eucalyptus (Goffner et al., 1992). Included within this clade were four CADs from grasses; *Bmr6*, rice OsCAD2, sugarcane (*Saccharum officinarum*) SoCAD, and ZmCAD2; the gene encoding ZmCAD2 is tightly linked to the *Bm1* locus of maize. Although *SbCAD4* was the most similar CAD to *Bmr6* in the sorghum genome, it was not found within this clade. The monocot and dicot sequences appear in separate groups within this clade. The loblolly pine and *Selaginella* CAD were also present in this clade and appeared basal to both monocot and dicot sequences. This analysis indicates that there is an evolutionarily conserved function of these CAD proteins in lignin synthesis.

SbCAD3 to *SbCAD7* form a clade with AtCAD2, AtCAD3, and AtCAD6 to AtCAD9. Within this clade is the aspen sinapyl aldehyde dehydrogenase, which has been shown to catalyze the reduction of phenolic aldehydes to alcohols (Li et al., 2001; Bomati and Noel, 2005). *SbCAD1*, CrCAD from *Chlamydomonas*, and PpCAD from *Physcomitrella* were basal to CAD2 and CAD-like clades. AtCAD1 from Arabidopsis and EgCAD1 from eucalyptus resided outside the other clades.

Expression of *Bmr6* and *SbCAD4*

Recently, maize *bm1* was associated with repressed expression of several CAD genes, including *ZmCAD2* (Shi et al., 2006; Guillaumie et al., 2007). Reverse transcription quantitative PCR (RT-qPCR) was used

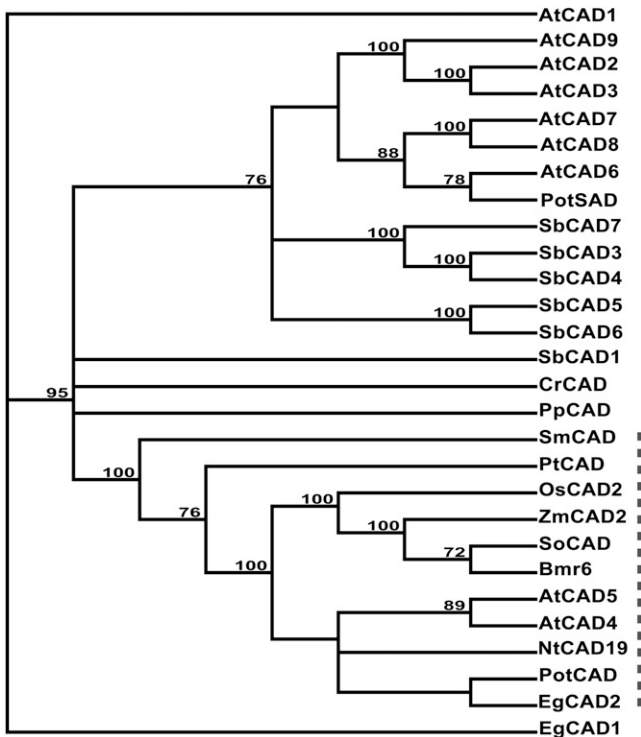


Figure 4. Phylogenetic analysis of CAD sequences. A phylogenetic tree was created based on predicted amino acids for putative and experimentally demonstrated CADs. The tree was constructed using the Neighbor-Joining method, and the Bootstrap method (1,000 repetitions) was used to estimate the certainty of the branch topography (values given). The GenBank accession number for each amino acid sequence is provided following the name, except for Arabidopsis, *Chlamydomonas*, *Physcomitrella*, *Selaginella*, and *Sorghum* sequences, whose sequence designation is from their respective genome project. Arabidopsis AtCAD1 (At1g72680), AtCAD2 (At2g21730), AtCAD3 (At2g21890), AtCAD4 (At3g19450), AtCAD5 (At4g34230), AtCAD6 (At4g37970), AtCAD7 (At4g37980), AtCAD8 (At4g37990), and AtCAD9 (At4g39330); aspen PotCAD (AAF43140) and PotSAD (AAK58693); *C. reinhardtii* CrCAD (CHLREDRAFT_190510); eucalyptus EgCAD1 (CAA61275) and EgCAD2 (CAA46585); loblolly pine PtCAD (CAA86073); maize ZmCAD2 (BM1 locus; NM_001112184); *P. patens* PpCAD (87951 scaffold_163:497997..49922); rice OsCAD2 (Os02g0187800); *S. moellendorffii* SmCAD (estExt_fgenesh2_pg_C_390191); sorghum SbCAD1 (Sb06g001430.1), SbCAD3 (Sb02g024210.1), SbCAD4 (Sb02g024190.1), SbCAD5 (Sb07g006090.1), SbCAD6 (Sb06g028240.1), and SbCAD7 (Sb02g024220.1); sugarcane SoCAD (CAA13177); and tobacco NtCAD19 (CAA44217). The dashed line indicates branches of tree containing CAD sequences whose function in monolignol biosynthesis has been genetically and/or biochemically demonstrated.

to examine the expression of *Bmr6* and *SbCAD4* in young internodes (see “Materials and Methods”) and to determine whether *bmr6* in sorghum has effects similar to *bm1* in maize. Expression was examined in wild-type, *bmr6*, *bmr12*, and *bmr6 bmr12* double mutant plants to determine whether either mutant or the double mutant combination affected the expression of *Bmr6* or *SbCAD4* (Fig. 5). *eIF4a1*, a housekeeping gene, was used as an internal control. *Bmr6*

expression in young internodes was significantly higher than *SbCAD4* for all genotypes, but only 4- to 5-fold higher in *bmr6* and *bmr6 bmr12* internodes. *Bmr6* expression was significantly decreased in *bmr6* and *bmr6 bmr12* compared to the wild type and *bmr12*, 20- and 15-fold, respectively (Fig. 5). Interestingly, *SbCAD4* expression was significantly increased in *bmr6* and *bmr6 bmr12* plants relative to the wild type and *bmr12*, 5- and 2.5-fold, respectively (Fig. 5). The increased *SbCAD4* expression in *bmr6* and *bmr6 bmr12* plants may highlight a compensatory mechanism for loss of CAD activity in *bmr6*.

Bmr6 and SbCAD4 Proteins

To detect the Bmr6 protein, polyclonal antibodies were raised against the recombinant Bmr6 protein (see “Materials and Methods”). Protein extracts from Atlas wild-type and *bmr6* internodes were separated by SDS-PAGE and probed with the polyclonal antibody (Fig. 6). The polyclonal antisera detected Bmr6 protein and three additional bands in the wild type, but the band corresponding to the Bmr6 protein was not detectable in Atlas *bmr6* (Fig. 6). The recombinant Bmr6 protein migrated slightly higher on SDS-PAGE than the endogenous Bmr6 (wild type) because of the addition of the His tag (Fig. 6). The polyclonal antisera also detected the recombinant SbCAD4 protein at concentrations equivalent to the recombinant Bmr6 protein (data not shown). The results were consistent with the mutation identified in *bmr6*, which would result in a truncated protein. However, the antibody failed to detect this truncated protein in extracts from *bmr6* plants, suggesting that the truncated *bmr6* protein was probably rapidly degraded.

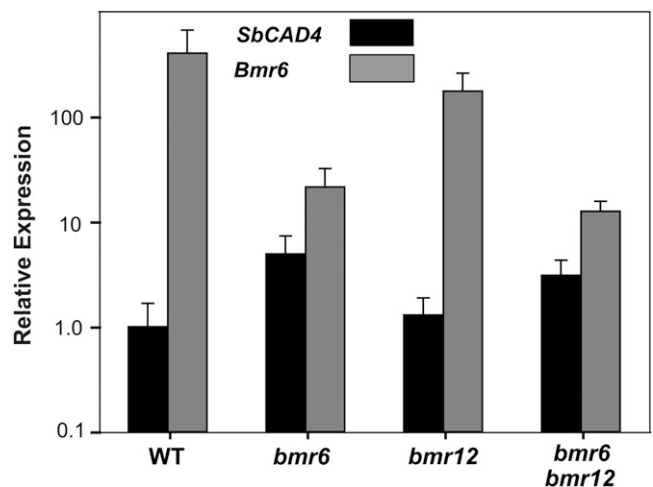


Figure 5. *Bmr6* and *SbCAD4* expression in young internodes. *Bmr6* and *SbCAD4* expression in young internodes was quantified by RT-qPCR for the following genotypes: the wild type (WT), *bmr6*, *bmr12*, and *bmr6 bmr12*. Relative expression levels were determined by the $\Delta\Delta C_t$ method, and *eIF4a1* was used as an internal standard. The data represent three replicates ($n = 3$).

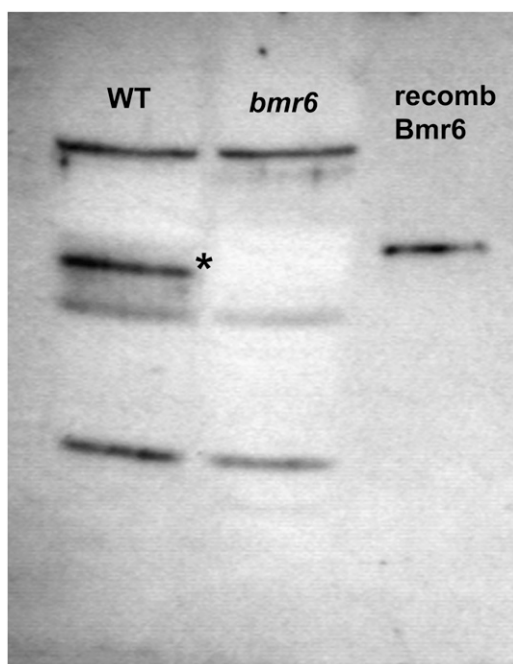


Figure 6. Immunoblot detection of Bmr6 from internodes. Protein extracts from wild-type (WT) and *bmr6* internodes were separated by SDS-PAGE, transferred to membrane, and probed with polyclonal antibodies raised against the recombinant (recomb) Bmr6 protein. The recombinant Bmr6 protein was loaded as a control. The asterisk denotes the band corresponding to Bmr6, which is absent in the *bmr6* extracts.

To examine the enzymatic activities of Bmr6 and SbCAD4 proteins, recombinant proteins were expressed in *Escherichia coli* and purified (see “Materials and Methods”). CAD activity was assayed using coniferyl alcohol and NADP⁺ as previously described (Palmer et al., 2008). To compare these two sorghum CAD proteins, enzyme kinetics for Bmr6 and SbCAD4 were determined for coniferyl alcohol (Table I). The K_m of SbCAD4 for coniferyl alcohol was almost 16-fold higher than that of Bmr6 and the V_{max} of SbCAD4 for coniferyl alcohol was 53-fold lower than that of Bmr6. The V_{max}/K_m of SbCAD4 for coniferyl alcohol was 842-fold lower than that of Bmr6. Assuming that recombinant SbCAD4 had comparable activity to the endogenous protein, these data suggest that coniferyl alcohol is probably not its preferred substrate.

The relative activities of recombinant Bmr6 and SbCAD4 proteins toward four cinnamyl alcohol substrates were assayed using coniferyl, coumaryl, caffeoyl, and sinapyl alcohol (see “Materials and Methods”). Bmr6 displayed significantly greater activity in comparison to SbCAD4 with all substrates (Fig. 7). For the coniferyl, coumaryl, and sinapyl alcohols, the activity of Bmr6 was 20- to 35-fold higher than that of SbCAD4 (Fig. 7). Neither enzyme showed robust activity with caffeoyl alcohol (Fig. 7). SbCAD4 showed slight activity for benzoyl alcohol, while Bmr6 had no detectable activity for this substrate (data not shown). Bmr6 activity was 2.2- and 2.6-fold greater,

respectively, when coumaryl and sinapyl alcohols were used as substrates compared to coniferyl alcohol as a substrate (Fig. 7).

In addition, the relative activities of recombinant Bmr6 and SbCAD4 proteins toward coniferyl and sinapyl aldehyde substrates were also determined (see “Materials and Methods”). Both Bmr6 and SbCAD4 had higher activities for the coniferyl and sinapyl aldehydes in comparison to the corresponding alcohols. The activity of Bmr6 was 2.5- and 34-fold higher than SbCAD4 for coniferyl and sinapyl aldehyde, respectively (Fig. 7). Bmr6 activity was still 2.5-fold greater when sinapyl aldehyde was used as a substrate compared to coniferyl aldehyde (Fig. 7). Interestingly, SbCAD4 had the highest activity for coniferyl aldehyde substrate, while Bmr6 had the highest activity for sinapyl aldehyde. Together, these results indicate that Bmr6 exhibits significantly stronger preference for the cinnamyl substrates required in lignin biosynthesis than SbCAD4.

Bmr6 and SbCAD4 Protein Structures

To examine how amino acid sequence differences between Bmr6 and SbCAD4 affect enzymatic activity, the structures of both proteins were modeled using the PotSAD, whose crystal structure containing the bound cofactor NADPH was published recently (Bomati and Noel, 2005) as a template. Using the predicted protein structures, AutoDock4 was used in conjunction with AutoDock Tools to predict the binding site for coniferyl aldehyde in the Bmr6 and SbCAD4 models. Amino acid side chains were left rigid during the simulation. The predicted substrate binding site for Bmr6 and predicted orientation of the substrate depicted in Figure 8A were consistent with the mechanism of alcohol dehydrogenases. However, the aldehyde group of the docked substrate was too distant for direct hydride transfer from C4 of the nicotinamide ring of NADP⁺ or for coordination with the catalytic zinc ion. This discrepancy was alleviated in part by adjustment of the active site side chains during substrate binding, a process that was modeled in AutoDock4. There were differences in side chains in the cofactor binding site between Bmr6 and PotSAD; hence, the cofactor atoms may be slightly misplaced in the model. A combination of adjustments to the position of NADP⁺ and active site side chains brought

Table I. Bmr6 and SbCAD4 kinetic parameters for coniferyl alcohol

The enzymatic velocities for Bmr6 and SbCAD4 were measured for a range of concentrations of coniferyl alcohol (Supplemental Fig. S2) to determine the enzyme kinetic parameters (see “Materials and Methods”; $n = 4$).

Enzyme Kinetic Parameters	Bmr6	SbCAD4
K_m (μM)	7.5 ± 1.2	117 ± 24
V_{max} ($\text{nmol s}^{-1} \text{mg protein}^{-1}$)	140 ± 7	2.6 ± 2.6
V_{max}/K_m ($\text{s}^{-1} \text{mg protein}^{-1}$)	1.87×10^{-2}	2.22×10^{-5}

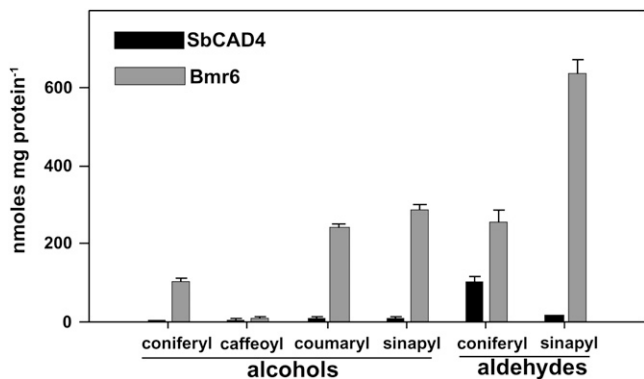


Figure 7. Enzyme activity of Bmr6 and SbCAD4 for different cinnamyl substrates. CAD activity was determined for SbCAD4 (black bars) and Bmr6 (gray bars) using NADP⁺ as the cofactor and coumaryl, coniferyl, caffeoyl, or sinapyl alcohol as the substrate. Alternatively, CAD activity was determined using NADPH as the cofactor and coniferyl or sinapyl aldehyde as the substrate. The activity is normalized to the amount of protein. Error bars denote SD ($n = 4$).

substrate and cofactor within sufficient proximity to support catalysis. In the model, Trp-119 was positioned to form a hydrophobic interaction with the aromatic ring of the substrate, which may help to stabilize the position of the substrate in the active site for catalysis.

Docking attempts using the model for SbCAD4 did not produce an orientation consistent with hydride transfer from the cofactor, even when side chain adjustments and slight misplacement of NADP⁺ were allowed. Inspection of the predicted binding pocket of SbCAD4 was potentially informative. Figure 8B shows a superposition of the active sites of Bmr6 and SbCAD4 with the position of bound substrate in Bmr6. In the SbCAD4 model, substrate was precluded from binding in the same orientation as observed in Bmr6 by the position of Tyr-93. On the opposite side of the substrate, Trp-56 was positioned at the bottom of the binding pocket toward the polar aldehyde group of the substrate. The proximity of polar and nonpolar groups would also be unfavorable for substrate binding in the SbCAD4 active site. Neighboring amino acids prevent the side chains of Tyr-93 and Trp-56 from moving far from the positions shown without large-scale adjustments to a number of amino acid positions (data not shown). These predicted differences in substrate docking between Bmr6 and SbCAD4 may explain the differences in enzymatic activity observed.

DISCUSSION

Bmr6 encodes a CAD that is phylogenetically distinct from other CADs within the sorghum genome and is involved in the lignification of sorghum tissues (Palmer et al., 2008). The nonsense mutation in *bmr6* (Gln to STOP) truncates the reading frame prior to the nucleotide binding and C-terminal catalytic domains

of the protein; consequently, the encoded protein is expected to be nonfunctional. Both immunological evidence (Fig. 6) and lack of detectable CAD activity in *bmr6* internodes (Palmer et al., 2008) support this hypothesis. However, reduced CAD activity has been reported in crude extracts from whole *bmr6* plants (Pillonel et al., 1991). This result suggests that one or more CAD-like proteins, such as SbCAD4, may be responsible for the residual CAD activity previously observed. The reduced lignin levels, accumulation of reddish pigmentation, and altered lignin composition, including the incorporation of phenolic aldehydes, observed in *bmr6* (Fig. 2; Pillonel et al., 1991; Palmer et al., 2008) indicate that Bmr6 is largely responsible for reducing phenolic aldehydes to alcohols for lignin biosynthesis, albeit not solely for monolignol biosynthesis in sorghum.

bmr6 and *bm1*

The sequence similarity between Bmr6 and ZmCAD2 indicate that ZmCAD2 is the gene product encoded by the *Bm1* locus as previously reported (Halpin et al.,

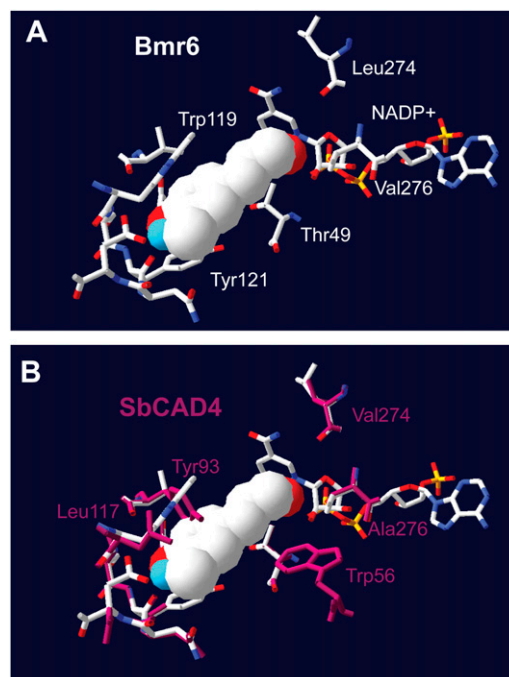


Figure 8. Predicted protein structure of Bmr6 and SbCAD4 containing the bound substrate. Amino acids 9 to 353 of Bmr6 aligned with the sequence for PtSAD with 51.9% sequence identity. Amino acids 8 to 353 of SbCAD4 sequence aligned with 60.8% identity to PtSAD. The positions of NADP⁺ and the two zinc ions were taken directly from the PtSAD structure and placed into each structural model. A, The active site of Bmr6 with coniferyl aldehyde bound, including the cofactor with the following depictions: carbon atoms (white), oxygen atoms (red), phosphorus atom (orange), and nitrogen atoms (blue). B, Model of Bmr6 with the active site for SbCAD4 overlaid in the purple. Only the amino acids within 5 Å of the docked substrate are represented.

1998). Both *bmr6* and *bm1* phenotypes have reduced CAD activity, reduced lignin levels, and incorporation of phenolic aldehydes into lignin (Pillonel et al., 1991; Provan et al., 1997; Halpin et al., 1998; Marita et al., 2003; Shi et al., 2006). However, our data indicate that there are dissimilarities between *bmr6* and *bm1* in gene expression and S:G lignin ratio. In *bmr6*, transcript levels of *SbCAD4* were not repressed; rather, *SbCAD4* transcript increased relative to the wild type (Fig. 5). In *bm1*, the expression of several CAD genes, including *ZmCAD2*, was repressed relative to the wild type (Shi et al., 2006; Guillaumie et al., 2007), which led to the suggestion that *Bm1* may encode a regulatory protein tightly linked to the *ZmCAD2* locus. Whether *bmr6* affects the expression of other lignin biosynthetic genes remains to be addressed. The S:G ratio was not altered in *bm1* (Halpin et al., 1998), but in *bmr6*, this ratio was reduced 2.4-fold compared to the wild type (Fig. 2A). The implications of this difference are unclear, but in other CAD-deficient plants, significant reductions in S:G ratio were observed similar to *bmr6* (Yahiaoui et al., 1998; Baucher et al., 1999; Sibout et al., 2005). Based on the data presented here and in other publications (Halpin et al., 1998; Kim et al., 2004; Sibout et al., 2005; Tobias and Chow, 2005), *ZmCAD2* likely catalyzes the last step in monolignol biosynthesis in maize. The absence of *ZmCAD2* expression could account for the reduced CAD activity in *bm1* (Halpin et al., 1998). Identifying the mutation either in *ZmCAD2* or another gene that is responsible for the *bm1* phenotype may be necessary to resolve this issue.

Bmr6 and Its Orthologs

Phylogenetic analysis indicates that *Bmr6* belongs to the CAD2 family (Goffner et al., 1992), whose functions as CADs have been genetically and/or biochemically demonstrated for several members. This CAD2 family appears to be evolutionarily conserved across vascular plants (Fig. 4). *Bmr6* sequence was more similar to CAD2 sequences from monocots, dicots, gymnosperms, and lycophytes (*Selaginella*) than to any other sequence in the sorghum genome. These results indicate that the last step in monolignol biosynthesis, the reduction of phenolic aldehydes into alcohol, is catalyzed by the CAD2 family and is functionally conserved across vascular plants. This evolutionary conservation is not entirely unexpected because lignin reinforces the xylem, which allows it to withstand negative pressure to conduct water from roots to shoots. The ability to transport water is one of the critical adaptations that allowed vascular plants to colonize land.

Although CAD activity is essential for native lignin formation, CAD2 exists as a single gene in the genomes of the grasses sorghum (this article) and rice (*Oryza sativa*; Tobias and Chow, 2005). In the draft genomes of poplar (*Populus* spp.), grape (*Vitis vinifera*), *Selaginella*, and *Medicago truncatula*, there also appears to be a single CAD2 gene (data not shown). In loblolly pine, a

mutant with a brown midrib phenotype has been isolated that abolishes CAD activity as indicated by allozyme analysis and *PtCAD* gene expression (Mackay et al., 1997). These data indicated that there is a single locus in the loblolly pine genome required for CAD activity and that mutation was linked to the *PtCAD* gene (Mackay et al., 1997), a member of the CAD2 family (Fig. 4). Similarly, the rice *gold hull and internode2* (*gh2*) mutant has also been shown to have a missense mutation in the rice CAD2 gene (Zhang et al., 2006). However, there are two CAD2 genes in Arabidopsis (*AtCAD4* and *AtCAD5*; Kim et al., 2004; Sibout et al., 2005), and a BLAST search of the draft of the soybean (*Glycine max*) genome also indicates that there are two CAD2 genes within its genome (data not shown). These data suggest that the ancestral CAD2 has been maintained as a single gene through the evolution of vascular plants until a recent duplication(s) in some dicot lineages.

Bmr6 Structure and Function

Clearly, *Bmr6* is a functional CAD that acts in monolignol biosynthesis (Fig. 7). A predicted reaction mechanism was recently published for *AtCAD5* and *AtCAD4* (Youn et al., 2006), and each shares 71% amino acid identity to *Bmr6*. Nearly all of the critical amino acids are conserved between *AtCAD5* and *Bmr6*, except for Asp-57 in the active site (Fig. 9). The proposed catalytic mechanism involves hydride transfer from NADPH to the aldehyde substrate coordinated by the catalytic zinc in the active site of the enzyme. Both Thr-49 and His-52 are critical to this process and participate in the proper orientation of the cofactor and in the hydride transfer (Youn et al., 2006), which are conserved in *Bmr6*. In contrast, within *Bmr6* and other grass CAD2 sequences, the conserved Asp-57 has been replaced by a His (Fig. 9), suggesting the change from the ancestral acidic amino acid, Asp or Glu, to the basic amino acid, His, might have some

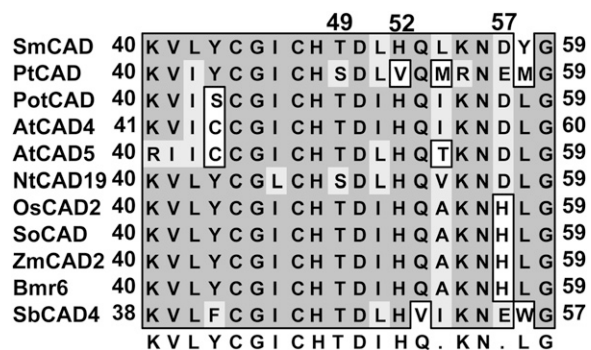


Figure 9. Alignment of amino acids involved in the proposed reaction mechanism. The amino acid sequences of the CAD2 clade and *SbCAD4* were aligned using ClustalW. Displayed are the amino acids found in the proposed active site, which is based on the crystal structure of *AtCAD5* (Youn et al., 2006).

functional significance. *Bmr6* was shown to have 2-fold higher activity with the coumaryl and sinapyl substrates, respectively, compared to the coniferyl substrates (Fig. 7), whereas *AtCAD5* displayed comparable activity with either substrate (Kim et al., 2004). The presence of a His at amino acid 57 could be responsible for this substrate preference, which may have an adaptive significance for grasses. Unlike dicots, grass cell walls contain significant amounts of ester and ether linked *p*-coumaric and ferulic acids that are separate from lignin polymers (Grabber et al., 1991; Boerjan et al., 2003). *p*-Coumaric acids are esterified to sinapyl alcohol prior to their incorporation into cell walls (Grabber and Lu, 2007), suggesting that significant amounts of sinapyl alcohol are required during cell wall biogenesis in grasses. Potentially, changes in the active site of grass CAD2 proteins have occurred to accommodate this differential need for specific monolignol precursors in the development of grass cell walls.

SbCAD4 Structure and Function

SbCAD4 is a member of the alcohol dehydrogenase superfamily but is distinctly different from the CAD2 clade that includes *Bmr6* (Fig. 4). The predicted structural model and substrate docking showed that in place of the Leu-58 found in the angiosperm CAD2s (Figs. 8 and 9), SbCAD4 contains a Trp-56, which has a larger, more rigid, hydrophobic side chain that is unlikely to favorably interact with the nearby hydrophilic aldehyde group of the substrate. More importantly, the position of Tyr-93 on the opposite end of the putative substrate binding site could obstruct or interfere with substrate binding (Fig. 8). Both of these amino acids are predicted to negatively impact substrate binding and could possibly explain the functional differences observed between *Bmr6* and SbCAD4 in vitro.

The endogenous function of SbCAD4 and other SbCADs or their substrates remain unclear. Based on the *bmr6* phenotype, the other CAD proteins have minor functions in lignin biosynthesis at best because there were significant alterations to phenylpropanoid metabolism and lignin observed in *bmr6* plants (Pillonel et al., 1991; Palmer et al., 2008). In vitro biochemical data indicated that the SbCAD4 protein has the ability to catalyze the conversion of hydroxycinnamoyl aldehydes to alcohols, albeit considerably less efficiently than *Bmr6* (Fig. 7; Table I). In the absence of *Bmr6*, sorghum plants incorporated limited amounts of monolignols and monolignals into their cell walls (Pillonel et al., 1991; Palmer et al., 2008), indicating that SbCAD4 and/or other SbCAD proteins were able to partially compensate for the loss of the *Bmr6* in monolignin biosynthesis. This conclusion assumes that phenolic aldehydes need to be enzymatically converted to alcohols to form the native linkages observed in lignin. Similar conclusions have been made about other CAD proteins that are not CAD2

proteins based on in vitro and in planta results in other plants (Goffner et al., 1998; Li et al., 2001; Kim et al., 2004; Bomati and Noel, 2005). In vitro many of these proteins have the ability to reduce a range of aldehydes to alcohols but do not fully compensate for the loss of CAD2 activity in lignin biosynthesis.

CONCLUSION

Here, we have presented evidence that *Bmr6* encodes the major CAD in sorghum. The type and position of the DNA lesion in *bmr6*, and the absence of the protein, confirm that *bmr6* is a null allele. *Bmr6* defines the major monolignol CAD protein in the grasses, which exists as a single locus in diploid grasses. *bmr6* demonstrates the potential for targeting this locus to reduce lignin content in grasses, with concomitant increases in forage digestibility by livestock and conversion to biofuels in lignocellulosic refineries. In the forage sorghum variety Atlas, *bmr6* increased in vitro neutral detergent fiber digestibility (IVNDFD) by 7% (Oliver et al., 2005) and reduced acid detergent lignin and Klason lignin by 33% and 15%, respectively (J. Pedersen, unpublished data), without an observed increase in lodging (Oliver et al., 2005). However, both dry matter yield and plant height were decreased by 9% (Oliver et al., 2005). The *Bmr6* locus, which has a significant impact on lignin content with relatively small effects on overall plant fitness, represents a potential target for traditional and transgenic approaches for bioenergy feedstock development.

MATERIALS AND METHODS

Preparation of Plant Materials

Genetic stocks were developed by crossing the recurrent parents Atlas, Wheatland, and RTx430 to the brown midrib sources N121 (*bmr6*) and F220 or F324 (*bmr12*, a gift from Robert Kalton) as described previously (Pedersen et al., 2006a, 2006b, 2008). Seeds were sown in a soil mix consisting of soil:peat moss:vermiculite:perlite:sand (4:1:1:1:1), grown in 28-cm pots under a 16-h-day regimen supplemented with high-pressure sodium lights and fertilized as needed (approximately every 7 d, 5 mL per pot) with a fertilizer containing 11:15:11 (N:P:K; Ferti-lome Gardener's Special). Plants were grown in the greenhouse during November, 2006; temperatures were maintained at 29°C to 30°C during the day and 26°C to 27°C during the night. Upon seedling emergence, the plants were thinned to two plants per pot. Following emergence of the inflorescence (approximately 40 d after planting), the top three internodes were harvested for gene expression analysis.

Relative Lignin Composition

Thioacidolysis followed by GC-MS was used to determine the relative lignin composition, and the subunits were identified (H-, G-, S-lignin, and other minor lignin components) based on mass spectra and quantified using major ions (*m/z*) previously published (Palmer et al., 2008). The Atlas ground stem material (Wiley mill, 1-mm screen) was washed, extracted, derivatized, and analyzed as previously described (Palmer et al., 2008).

Amplification and Sequencing

Sorghum (*Sorghum bicolor*) DNA was extracted from sorghum leaf tissue using a cetyl-trimethyl-ammonium bromide-based DNA extraction buffer

(Rogers and Bendich, 1985). PCR primers were designed for the CAD genes based on predicted gene models from the Sorghum Genome Project (<http://www.phytozome.net/sorghum>), and amplification was performed using 5' mastermix (Eppendorf), 10 μ M primer (Supplemental Table S1), and 100 ng of DNA. The Genomic Core Research Facility at the University of Nebraska performed automated DNA sequencing of amplification products. DNA sequence assembly and bioinformatic analysis were performed using the MacVector version 10.0 software package. For the CAPS marker for *Bmr6* (Supplemental Table S1), 2 μ L of 20 μ L PCR reaction were digested with 2.5 units of *Bsa*I and analyzed by agarose gel electrophoresis.

RT-qPCR

RNA was extracted from young internodes as previously described (Suzuki et al., 2004). Total RNA was treated with RQ1 RNase-free DNase (Promega). One microgram of DNase-treated total RNA from each sample was reverse transcribed using an anchored oligo(dT) primer and the Transcriptor First Strand cDNA kit (Roche Diagnostics). Real-time PCR was performed using the Sybr Green kit and an ABI 7000 instrument (Applied Biosystems). Primers for *Bmr6*, *SbCAD4*, and elongation factor (*SbElF4a1*) were designed with primer express software (Applied Biosystems; Supplemental Table S1) and optimized. Thermal cycling parameters consisted of a 10-min hold at 95°C to activate the enzyme, followed by 40 cycles of denaturing at 95°C for 15 s, and anneal/extend at 60°C for 1 min. Expression of mRNA was calculated using the threshold cycle (Ct) value. The values for *Bmr6* and *SbCAD4* were normalized to the housekeeping gene *elF4a1* (Sb04g003390). Relative expression was calculated using the $\Delta\Delta C_t$ method. These reactions were performed in triplicate. No template and RNA only (no RT reaction) negative controls were performed to ensure that DNA contamination was not present. These primer pairs were validated over a 6-log dilution range to determine that all three primer pairs had amplification efficiencies near 100%. One-fiftieth of the RT reactions was used for real-time PCR amplification.

Protein Expression and Characterization

The entire coding regions of *Bmr6* and *SbCAD4* were cloned into the pET30a vector (Novagen) as *Kpn*I-*Hind*III fragments from University of Georgia EST clones OX1_59_B11 and OX1_61_H04 (Supplemental Table S1). These vectors were freshly transformed into Rossetta R2 *Escherichia coli* cells for protein expression. Cultures were grown to log phase from a single colony at 37°C, and then protein expression was induced using 0.5 mM isopropylthio- β -galactoside at 20°C for approximately 18 h. Soluble proteins were extracted using sonication at 20 W with a 10-s pulse following a 30-s rest interval for 3 min. The expressed proteins, which contained N-terminal 6-His-tags, were isolated by affinity purification on a nickel column and eluted with imidazole. Induction of the expressed proteins and protein purification was monitored by SDS-PAGE. Polyclonal antibodies against *Bmr6* were prepared in rabbits by Cocalico Biologicals. Samples were separated on a 12% SDS gel. After separation, the gel was washed in transfer buffer [10 mM 3-(cyclohexylamino) propanesulfonic acid, pH 11.0, and 8% methanol] for 10 min and then transferred to a nitrocellulose membrane in a semidry blotter for 60 min at 2 mA/cm² of membrane. Following transfer, the membrane was stained with Ponceau S to verify the quality of transfer and then blocked with 3% nonfat dry milk in TBST (TBS + 0.5% Tween 20) for 1 h. The membrane was probed with primary antibody (polyclonal rabbit anti-rBmr6) at a 1:1,000 dilution in TBST + 3% milk for 1 h and then washed three times for 5 min each with TBST. The secondary antibody (goat anti-rabbit IgG + horseradish peroxidase; Sigma-Aldrich A-0545) was used at a dilution of 1:5,000 in TBST + 3% milk for 1 h. The membrane was then washed twice in TBST for 5 min each and once in TBS + 0.5 M NaCl for 5 min. Secondary antibody was detected using Amersham ECL western blotting reagent (GE Healthcare) and blue film.

CAD Enzymatic Activity

To compare enzyme activity on various substrates, each substrate was measured using standardized reaction conditions that consisted of 200 μ M substrate, 200 μ M NADP⁺ or NADPH, 100 mM Tris-HCl at pH 8.8, and 10 or 20 μ L of *Bmr6* or *SbCAD4*, which had been previously diluted with buffer (100 mM Tris-HCl, pH 7.5, 5 mM dithiothreitol, and 5% ethylene glycol) to ensure appropriate levels of activity for the assay. Enzyme dilutions were prepared immediately prior to use from concentrated aliquots that were stored at -80°C. Deionized water was added to keep total reaction volume constant at

200 μ L, and reactions were replicated four times. Activity was monitored using a 96-well plate reader (SpectraMax Plus 384; Molecular Devices) that was set to read A_{340} and 400 nm, which were sensitive to NADPH and aldehyde production, respectively. Total time between enzyme addition to a well and placement into the plate reader was monitored and kept constant at 35 s. Data were analyzed using KaleidaGraph 4.0 (Synergy Software) and SAS for Windows 9.1 (SAS Institute). The method of linear least squares (PROC REG) was used to fit a simple two parameter model to the optical density data, which provided an estimate of the aldehyde production rate. Kinetic parameters K_m and V_{max} were calculated using nonlinear least squares under the general curve fit procedure in KaleidaGraph 4.0.

Protein Modeling

Models of *Bmr6* and *SbCAD4* were created using SWISS-MODEL (Schwede et al., 2003). For both proteins, *Populus tremuloides* sinapyl alcohol dehydrogenase (Protein Data Bank ID 1YQD; Bomati and Noel, 2005) was selected as the template for structural modeling. This structure was chosen over the structure of AtCAD5 due to the presence of NADP⁺ in the PotSAD structure. The structure of coniferyl aldehyde was generated using PC model 9.1 software (Serena Software). Gasteiger charges were generated, and the structure was optimized using the same software package. This energy minimized coniferyl aldehyde structure was docked to our structural models of *Bmr6* and *SbCAD4* using AutoDock4 and AutoDock tools (Morris et al., 1998; Huey et al., 2007).

Supplemental Data

The following materials are available in the online version of this article.

Supplemental Figure S1. Protein alignment of *Bmr6*, *SbCAD4*, and CAD2 sequences.

Supplemental Figure S2. *Bmr6* and *SbCAD4* enzyme velocities for coniferyl alcohol.

Supplemental Table S1. Primer sequences used in this article.

ACKNOWLEDGMENTS

We thank Tammy Gries, Patrick O'Neill, John Toy, and Peter Madzellan for their technical assistance on experiments presented in this manuscript and Heather Van Buskirk for critically reviewing this manuscript. We thank Uyen Chu and James Takacs for the generous gift of the cinnamyl alcohol substrates. The identification of *bmr6* (Saballos et al., 2009) was published while this manuscript was under review.

Received January 29, 2009; accepted April 6, 2009; published April 10, 2009.

LITERATURE CITED

- Akin DE, Rigsby LL, Hanna WW, Lyon CE (1993) In vitro digestion and textural strength of rind and pith of normal and brown midrib stems. *Anim Feed Sci Technol* **43**: 303–314
- Anterola AM, Lewis NG (2002) Trends in lignin modification: a comprehensive analysis of the effects of genetic manipulations/mutations on lignification and vascular integrity. *Phytochemistry* **61**: 221–294
- Baucher M, Bernard-Vailhe MA, Chabbert B, Besle JM, Opsomer C, Van Montagu M, Botterman J (1999) Down-regulation of cinnamyl alcohol dehydrogenase in transgenic alfalfa (*Medicago sativa* L.) and the effect on lignin composition and digestibility. *Plant Mol Biol* **39**: 437–447
- Bigami M, Vitelli A, Di Muccio A, Terlizze M, Calcagnile A, Zapponi GA, Lohman PHM, Den Engelse L, Dogliotti E (1988) Relationship between specific alkylated bases and mutations at two gene loci induced by ethylnitrosourea and diethyl sulfate in CHO cells. *Mutat Res* **193**: 43–51
- Boerjan W, Ralph J, Baucher M (2003) Lignin biosynthesis. *Annu Rev Plant Biol* **54**: 519–546
- Bomati EK, Noel JP (2005) Structural and kinetic basis for substrate selectivity in *Populus tremuloides* sinapyl alcohol dehydrogenase. *Plant Cell* **17**: 1598–1611

- Bout S, Vermerris W** (2003) A candidate-gene approach to clone the sorghum Brown midrib gene encoding caffeic acid O-methyltransferase. *Mol Genet Genomics* **269**: 205–214
- Bucholtz DL, Cantrell RP, Axtell JD, Lechtenberg VL** (1980) Lignin biochemistry of normal and brown midrib mutant sorghum. *J Agric Food Chem* **28**: 1239–1241
- Carpita N, McCann C** (2000) The cell wall. In BB Buchanan, W Gruissem, RL Jones, eds, *Biochemistry and Molecular Biology of Plants*. American Society of Plant Physiologists, Rockville, MD, pp 52–109
- Chang MC** (2007) Harnessing energy from plant biomass. *Curr Opin Chem Biol* **11**: 677–684
- Chen F, Dixon RA** (2007) Lignin modification improves fermentable sugar yields for biofuel production. *Nat Biotechnol* **25**: 759–761
- Cherney DJ, Patterson JA, Johnson KD** (1990) Digestibility and feeding value of pearl millet as influenced by the brown-midrib, low-lignin trait. *J Anim Sci* **68**: 4345–4351
- Dixon RA, Chen F, Guo D, Parvathi K** (2001) The biosynthesis of monolignols: a “metabolic grid”, or independent pathways to guaiacyl and syringyl units? *Phytochemistry* **57**: 1069–1084
- Ezeji TC, Qureshi N, Blaschek HP** (2007) Bioproduction of butanol from biomass: from genes to bioreactors. *Curr Opin Biotechnol* **18**: 220–227
- Goffner D, Joffroy I, Grimapettenati J, Halpin C, Knight ME, Schuch W, Boudet AM** (1992) Purification and characterization of isoforms of cinnamyl alcohol-dehydrogenase from eucalyptus xylem. *Planta* **188**: 48–53
- Goffner D, Van Doorselaere J, Yahiaoui N, Samaj J, Grima-Pettenati J, Boudet AM** (1998) A novel aromatic alcohol dehydrogenase in higher plants: molecular cloning and expression. *Plant Mol Biol* **36**: 755–765
- Grabber JH, Jung GA, Hill RR** (1991) Chemical-composition of parenchyma and sclerenchyma cell-walls isolated from orchardgrass and switchgrass. *Crop Sci* **31**: 1058–1065
- Grabber JH, Lu F** (2007) Formation of syringyl-rich lignins in maize as influenced by feruloylated xylans and p-coumaroylated monolignols. *Planta* **226**: 741–751
- Grima-Pettenati J, Feuillet C, Goffner D, Borderies G, Boudet AM** (1993) Molecular cloning and expression of a *Eucalyptus gunnii* cDNA clone encoding cinnamyl alcohol dehydrogenase. *Plant Mol Biol* **21**: 1085–1095
- Guillaumie S, Pichon M, Martinant JP, Bosio M, Goffner D, Barriere Y** (2007) Differential expression of phenylpropanoid and related genes in brown-midrib bm1, bm2, bm3, and bm4 young near-isogenic maize plants. *Planta* **226**: 235–250
- Gupta SC** (1995) Allelic relationships and inheritance of brown midrib trait in sorghum. *J Hered* **86**: 72–74
- Halpin C, Holt K, Chojecki J, Oliver D, Chabbert B, Monties B, Edwards K, Barakate A, Foxon GA** (1998) Brown-midrib maize (bm1)—a mutation affecting the cinnamyl alcohol dehydrogenase gene. *Plant J* **14**: 545–553
- Halpin C, Knight ME, Foxon GA, Campbell MM, Boudet AM, Boon JJ, Chabbert B, Tollier MT, Schuch W** (1994) Manipulation of lignin quality by down-regulation of cinnamyl alcohol dehydrogenase. *Plant J* **6**: 339–350
- Huey R, Morris GM, Olson AJ, Goodsell DS** (2007) A semiempirical free energy force field with charge-based desolvation. *J Comput Chem* **28**: 1145–1152
- Jorgenson LR** (1931) Brown midrib in maize and its linkage relations. *J Am Soc Agron* **23**: 549–557
- Jung HG, Mertens DR, Buxton DR** (1998) Forage quality variation among maize inbreds: In vitro fiber digestion kinetics and prediction with NIPS. *Crop Sci* **38**: 205–210
- Jung HJG, Ni W** (1998) Lignification of plant cell walls: Impact of genetic manipulation. *Proc Natl Acad Sci USA* **95**: 12742–12743
- Kim SJ, Kim MR, Bedgar DL, Moineuddin SGA, Cardenas CL, Davin LB, Kang CL, Lewis NG** (2004) Functional reclassification of the putative cinnamyl alcohol dehydrogenase multigene family in Arabidopsis. *Proc Natl Acad Sci USA* **101**: 1455–1460
- Knight ME, Halpin C, Schuch W** (1992) Identification and characterization of cDNA clones encoding cinnamyl alcohol dehydrogenase from tobacco. *Plant Mol Biol* **19**: 793–801
- Li LG, Cheng XF, Leshkevich J, Umezawa T, Harding SA, Chiang VL** (2001) The last step of syringyl monolignol biosynthesis in angiosperms is regulated by a novel gene encoding sinapyl alcohol dehydrogenase. *Plant Cell* **13**: 1567–1585
- Li X, Weng JK, Chapple C** (2008) Improvement of biomass through lignin modification. *Plant J* **54**: 569–581
- Mackay JJ, Liu WW, Whetten R, Sederoff RR, Omalley DM** (1995) Genetic analysis of cinnamyl alcohol dehydrogenase in loblolly pine: single-gene inheritance, molecular characterization and evolution. *Mol Genet* **247**: 537–545
- Mackay JJ, O'Malley DM, Presnell T, Booker FL, Campbell MM, Whetten RW, Sederoff RR** (1997) Inheritance, gene expression, and lignin characterization in a mutant pine deficient in cinnamyl alcohol dehydrogenase. *Proc Natl Acad Sci USA* **94**: 8255–8260
- Marita JM, Vermerris W, Ralph J, Hatfield RD** (2003) Variations in the cell wall composition of maize brown midrib mutants. *J Agric Food Chem* **51**: 1313–1321
- Morris GM, Goodsell DS, Halliday RS, Huey R, Hart WE, Belew RK, Olson AJ** (1998) Automated docking using a Lamarckian genetic algorithm and empirical binding free energy function. *J Comput Chem* **19**: 1639–1662
- Oliver AL, Grant RJ, Pedersen JE, O'Rear J** (2004) Comparison of brown midrib-6 and -18 forage sorghum with conventional sorghum and corn silage in diets of lactating dairy cows. *J Dairy Sci* **87**: 637–644
- Oliver AL, Pedersen JE, Grant RJ, Klopfenstein TJ** (2005) Comparative effects of the sorghum bmr-6 and bmr-12 genes: I. Forage sorghum yield and quality. *Crop Sci* **45**: 2234–2239
- Palmer NA, Sattler SE, Saathoff AJ, Funnell D, Pedersen JE, Sarath G** (2008) Genetic background impacts soluble and cell wall-bound aromatics in brown midrib mutants of sorghum. *Planta* **229**: 115–127
- Pedersen JE, Funnell DL, Toy JJ, Oliver AL, Grant RJ** (2006a) Registration of ‘Atlas bmr-12’ forage sorghum. *Crop Sci* **46**: 478
- Pedersen JE, Funnell DL, Toy JJ, Oliver AL, Grant RJ** (2006b) Registration of twelve grain sorghum genetic stocks near-isogenic for the brown midrib genes bmr-6 and bmr-12. *Crop Sci* **46**: 491–492
- Pedersen JE, Toy JJ, Funnell DL, Sattler SE, Oliver AL, Grant RA** (2008) Registration of BN611, AN612, BN612, and RN613 sorghum genetic stocks with stacked bmr-6 and bmr-12 genes. *Journal of Plant Registrations* **2**: 258–262
- Pillonel C, Mulder MM, Boon JJ, Forster B, Binder A** (1991) Involvement of cinnamyl-alcohol dehydrogenase in the control of lignin formation in *Sorghum bicolor* L Moench. *Planta* **185**: 538–544
- Porter KS, Axtell JD, Lechtenberg VL, Colenbrander VF** (1978) Phenotype, fiber composition, and in vitro dry matter disappearance of chemically induced brown midrib (bmr) mutants of sorghum. *Crop Sci* **18**: 205–208
- Provan GJ, Scobbie L, Chesson A** (1997) Characterisation of lignin from CAD and OMT deficient Bm mutants of maize. *J Sci Food Agric* **73**: 133–142
- Ralph J, MacKay JJ, Hatfield RD, O'Malley DM, Whetten RW, Sederoff RR** (1997) Abnormal lignin in a loblolly pine mutant. *Science* **277**: 235–239
- Rogers SO, Bendich AJ** (1985) Extraction of DNA from milligram amounts of fresh, herbarium and mummified plant tissues. *Plant Mol Biol* **5**: 69–76
- Roman-Leshkov Y, Barrett CJ, Liu ZY, Dumesic JA** (2007) Production of dimethylfuran for liquid fuels from biomass-derived carbohydrates. *Nature* **447**: 982–985
- Saballos A, Ejeta G, Sanchez E, Kang C, Vermerris W** (2009) A genome-wide analysis of the cinnamyl alcohol dehydrogenase family in sorghum [*Sorghum bicolor* (L.) Moench] identifies SbCAD2 as the Brown midrib6 gene. *Genetics* **181**: 783–795
- Sarath G, Mitchell RB, Sattler SE, Funnell D, Pedersen JE, Graybosch RA, Vogel KP** (2008) Opportunities and roadblocks in utilizing forages and small grains for liquid fuels. *J Ind Microbiol Biotechnol* **35**: 343–354
- Schmer MR, Vogel KP, Mitchell RB, Perrin RK** (2008) Net energy of cellulosic ethanol from switchgrass. *Proc Natl Acad Sci USA* **105**: 464–469
- Schwede T, Kopp J, Guex N, Peitsch MC** (2003) SWISS-MODEL: an automated protein homology-modeling server. *Nucleic Acids Res* **31**: 3381–3385
- Shi C, Koch G, Ouzunova M, Wenzel G, Zein I, Lubberstedt T** (2006) Comparison of maize brown-midrib isogenic lines by cellular UV-microspectrophotometry and comparative transcript profiling. *Plant Mol Biol* **62**: 697–714
- Sibout R, Eudes A, Mouille G, Pollet B, Lapierre C, Jouanin L, Seguin A** (2005) Cinnamyl alcohol dehydrogenase-C and -D are the primary genes

- involved in lignin biosynthesis in the floral stem of *Arabidopsis*. *Plant Cell* **17**: 2059–2076
- Suzuki Y, Kawazu T, Koyama H** (2004) RNA isolation from siliques, dry seeds, and other tissues of *Arabidopsis thaliana*. *Biotechniques* **37**: 542
- Tobias CM, Chow EK** (2005) Structure of the cinnamyl-alcohol dehydrogenase gene family in rice and promoter activity of a member associated with lignification. *Planta* **220**: 678–688
- Vermerris W, Saballos A, Ejeta G, Mosier NS, Ladisch MR, Carpita NC** (2007) Molecular breeding to enhance ethanol production from corn and sorghum stover. *Crop Sci (Suppl 3)* **47**: S142–S153
- Vignols F, Rigau J, Torres MA, Capellades M, Puigdomenech P** (1995) The brown midrib3 (*bm3*) mutation in maize occurs in the gene encoding caffeic acid *O*-methyltransferase. *Plant Cell* **7**: 407–416
- Vogel KP, Jung HJG** (2001) Genetic modification of herbaceous plants for feed and fuel. *Crit Rev Plant Sci* **20**: 15–49
- Yahiaoui N, Marque C, Myton KE, Negrel J, Boudet AM** (1998) Impact of different levels of cinnamyl alcohol dehydrogenase down-regulation on lignins of transgenic tobacco plants. *Planta* **204**: 8–15
- Youn B, Camacho R, Moinuddin SGA, Lee C, Davin LB, Lewis NG, Kang CH** (2006) Crystal structures and catalytic mechanism of the *Arabidopsis* cinnamyl alcohol dehydrogenases AtCAD5 and AtCAD4. *Org Biomol Chem* **4**: 1687–1697
- Zhang KW, Qian Q, Huang ZJ, Wang YQ, Li M, Hong LL, Zeng DL, Gu MH, Chu CC, Cheng ZK** (2006) *GOLD HULL AND INTERNODE2* encodes a primarily multifunctional cinnamyl-alcohol dehydrogenase in rice. *Plant Physiol* **140**: 972–983